Adaptive Power Control for Underwater Acoustic Communications

Parastoo Qarabaqi and Milica Stojanovic
Department of Electrical and Computer Engineering
Northeastern University
Boston, Massachusetts 02115
Email: {qarabaqi, millitsa}@ece.neu.edu

***Abstract*—Experimental measurements of shallow water acoustic channels show that the received signal power varies over time as the channel experiences fading. This fact motivates the use of adaptive power (or rate) control as a way to improve the system performance or save the transmit power. In a system with adaptive power control, the transmitter adjusts its power so that the received power remains at a pre-specified level whenever possible, or it shuts down when the channel conditions deteriorate beyond some point. Adaptive power control relies on feedback by which the receiver informs the transmitter of the present channel state. The transmitter can then predict the next state and adjust its power accordingly. This procedure will be effective if the channel variations are slow enough for the feedback mechanism to be implemented. In this paper, we investigate the feasibility of adaptive power control for underwater acoustic (UWA) communications using data recorded during the Surface Processes Acoustic Communications Experiment (SPACE) which was conducted off the coast of New England in a shallow water channel over a range of 1 km. The slow variations of the locally-averaged received power are shown to exhibit properties of a log-normally distributed autoregressive (AR) process with a coherence time on the order of several seconds. Adaptive prediction of the gain is applied to experimental data, demonstrating the feasibility of power control and indicating that substantial savings in average power are available over extended periods of time (about 9 dB over several hours). These values are also confirmed by a theoretical analysis.**

I. Introduction

Experimental measurements (Fig. 1) show that the received signal power in an underwater acoustic channel varies in time as the channel experiences fading. To ensure satisfactory reception in such conditions, a conventional system is designed to include a fading margin. In other words, the transmit power is set to a higher value than what is deemed necessary by a nominal acoustic propagation model. By transmitting at a higher power at all times, it is guaranteed that the received power will be sufficient in a certain percentage of time. However, this approach has two drawbacks: (1) when the channel conditions are favorable, more power is used than necessary, and (2) when the channel deteriorates beyond some point, transmissions are made in vain. These facts motivate the use of adaptive power (or rate) control as a way to improve the system performance or save the transmit power. Knowledge of the channel statistics is key to designing an efficient power control method; however, at present there are no widely accepted models for the acoustic channel fading. Nonetheless, research is active on this topic, and recent studies have proposed several models based on experimental measurements [1] - [7].

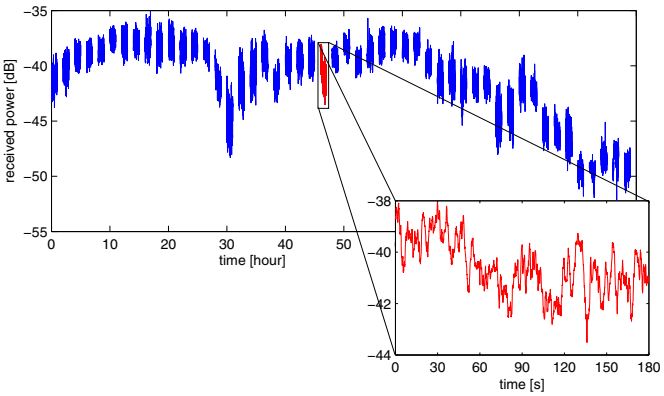

Fig. 1. *Normalized received power over several hours, and a zoomed-in illustration of the received power variations over three minutes.*

Statistical channel characterization addresses two aspects: the probability distribution and the time-coherence properties. While knowledge of both types of information can be exploited for designing a power control method, the latter is of crucial importance, since power control can be applied only when the coherence time of the channel is long enough compared to the round-trip delay. Power control algorithms have been widely studied for wireless radio and satellite channels. Examples include references [8] - [10], where an autoregressive moving average model with an auxiliary input process (e.g. Gaussian) is used to model the channel fading. However, no comparable work has been carried out for UWA channels.

In the present work, experimental data are used to model the statistics of a shallow water channel. The locally-averaged power gain, expressed on a logarithmic scale (in dB), which can be interpreted as the large-scale slow fading component, is modeled as an autoregressive (AR) random process whose coherence time is found to be on the order of a few seconds.

Two approaches are considered for adaptive power control. One approach simply uses the outdated estimate of the channel's power gain, whereas the other incorporates knowledge of the AR nature of the gain to predict its value one travel time ahead. For the experimental channel at hand, which proved to be slowly varying, both approaches are shown to enable power savings of several dB.

The rest of the paper is organized as follows. In Section II, the problem is formulated and experimental data are described. In Section III, theoretical bounds on power savings available in conditions of log-normal fading with known AR parameters are given. Section IV presents the results of experimental data processing which show the feasibility of adaptive power control using channel state prediction. Conclusions are summarized in Section V.

II. System Description

In this section, we define the parameters that will be used throughout the paper, and we describe the experimental data.

A. The Gain

A practical UWA system operates in a finite frequency bandwidth B centered around some frequency f_c. Assuming that the transmitted signal has a flat power spectral density S_T, its power is $P_T = S_T B$. Given the channel transfer function $\tilde{H}(f,t)$ at some time t, the power spectral density of the received signal will be $\tilde{S}_R(f,t) = S_T|\tilde{H}(f,t)|^2$. The corresponding received power is

$$\tilde{P}_R(t) = \int_{-\infty}^{+\infty} \tilde{S}_R(f,t)df = P_T\tilde{G}(t) \qquad (1)$$

where

$$\tilde{G}(t) = \frac{1}{B}\int_{f_c-B/2}^{f_c+B/2} |\tilde{H}(f,t)|^2 df \qquad (2)$$

represents the *instantaneous* power gain. We denote the instantaneous power gain on the dB scale by $\tilde{g}(t) = 10\log\tilde{G}(t)$. Throughout the paper, lower case quantities are used to denote the parameters in dB.

Fig. 1 shows the variation of the instantaneous received power with time, as observed from the experimental data. The transmit power was kept constant during the experiment. The figure thus demonstrates a scaled version of the instantaneous power gain. The process appears to have a slowly varying local average with superimposed faster variations.

While a simple feedback mechanism cannot aspire to predict the fast variations of the instantaneous power, such as those caused by scattering, it may be possible to predict the slower variations of the *locally averaged* power. We define the locally averaged power gain, or simply the gain, as

$$g(t) = \frac{1}{T_w}\int_{t-T_w}^{t} \tilde{g}(s)ds \qquad (3)$$

where T_w is the averaging window.

Fig. 2 illustrates a feedback process where the receiver provides the transmitter with the gain $g(t)$ through a feedback channel. The averaging window T_w is chosen to be 2 seconds in this case. The feedback signals are transmitted every t_f seconds and used to predict the gain t_l seconds ahead. In a practical power control system, the prediction lag t_l is chosen to be at least the round-trip delay, which is the time by which the feedback signal will be outdated once the adjusted transmit signal arrives at the receiver. For the hypothetical 2 km long channel of Fig. 2, t_l is chosen to be equal to the round-trip delay of 2.6 seconds. For the illustrated system, two feedback signals are transmitted during the prediction lag time ($t_f = t_l/2$).

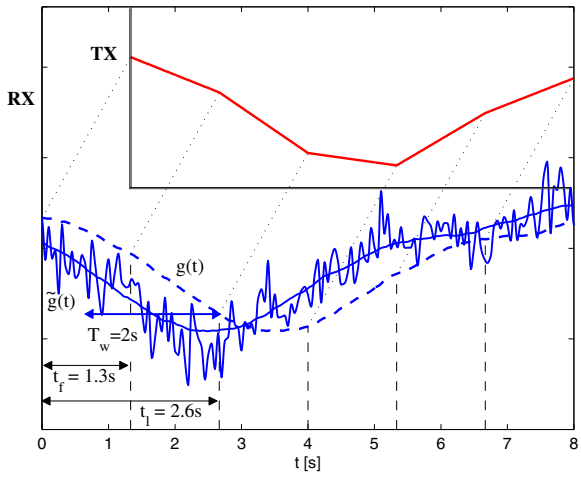

Fig. 2. *The receiver feeds $g(t)$ back to the transmitter.*

B. Experiment Description

The SAPCE'08 data were collected south of the coast of Martha's Vineyard in Massachusetts, in the fall of 2008. The transmitted signal was a PN sequence of length 4095, BPSK modulated repeatedly onto a carrier frequency of 12.5 kHz at rate $R = 6.5$ kbps. The signal was transmitted for three minutes every two hours. We refer to the active three-minute interval of each two hour period as one epoch. The experiment lasted for 15 days. Three receivers located at distances of 60 m, 200 m and 1000 m from the transmitter recorded the signals.

The data were first used to estimate the channel response. An adaptive RLS algorithm was employed. The so-obtained channel estimates $\tilde{H}(f,t)$ were used to determine the instantaneous gain (2). Finally, the average gain $g(t)$ was obtained by local averaging (3).

We treat each epoch as one realization of a single process and combine adjacent epochs after appropriate shifting to obtain a long record.

From the so-obtained long record, we first study the statistical properties of the experimental gain. More specifically, we inspect the probability density function (pdf) and the auto-correlation function of the gain. The averaging window T_w is set to 2 seconds. We will discuss the choice of T_w in more details in Section IV, where we show that an averaging window of 2 seconds is in fact a reasonable choice in light of minimizing the prediction error.

Fig. 3 shows the histogram of the gain $g(t)$ and a Gaussian pdf with mean $\bar{g}$ and variance σ^2 estimated from the data. The figure implies that $G(t)$ can be modeled as a log-normally distributed process. Fig. 4 shows the auto-correlation of $g(t)$. The figure indicates a coherence time of several seconds which is long enough to support feedback over a 1 km acoustic link. Shown also in the figure are the auto-correlation functions

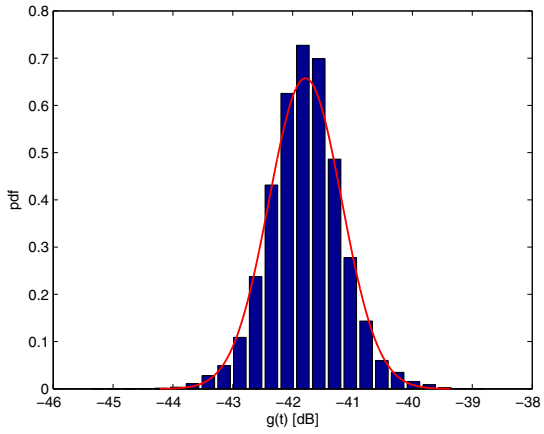

Fig. 3. *Histogram of $g(t)$ and a Gaussian fit.*

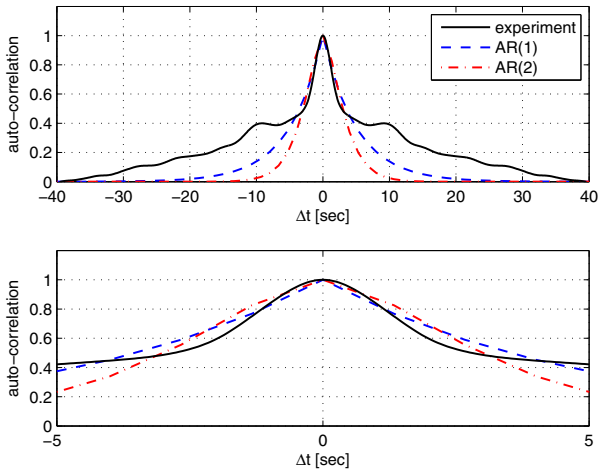

Fig. 4. *Auto-correlation of $g(t)$ and a zoomed-in plot of the auto-correlation function.*

corresponding to a first order and a second order AR process matched to the experimental data.

The parameters of the AR processes are estimated from experimental data using the Yule-Walker equations [12]. For $t_f = 1.3$ s, the resulting AR(1) parameter a_1 equals 0.77 and for the AR(2) process, $[a_1, a_2] = [0.92, -0.20]$. As emphasized by the zoomed-in plot, the AR models appear to be a good match for our experimental channel, especially for time differences of a few seconds.

Assuming that the gain obeys an AR process, linear prediction can be employed to adjust the transmit power level to suite the channel conditions; i.e., to implement adaptive power control.

III. Power Control: Theoretical Considerations

In this section, we look at theoretical gains that are achievable by adaptive power control assuming that the fading model is known. We first define the power control algorithm and then analyze its performance under the AR(1) and AR(2) models assuming a log-normal distribution for $G(t)$. In what follows, we will use G in place of $G(t)$ for simplicity. A method based on an outdated gain estimate is also considered as a benchmark.

While the log-normal distribution assumption enables analytical assessment of the achievable power savings, it does not restrict the proposed power control method. Log-normal behavior of the gain has been observed in other underwater channels (e.g. [11]) as well as in the present SPACE'08 experimental channel.

A. Description of the Algorithm

In a conventional system where no power control mechanism is applied, a fixed margin is introduced to ensure that the Signal to Noise Ratio (SNR) $\gamma = P_T G/P_N$ remains above a threshold γ_0 with probability $1 - P_{out}$, where P_N is the noise power and $P_{out} = P\{\gamma < \gamma_0\}$ is the outage probability. When the transmit power is constant, the outage probability is given by $P_{out} = P\{G < P_N\gamma_0/P_T\} = P\{G < G_{out}\}$. Let P_{T0} be the power needed to achieve γ_0 in the absence of fading ($G = \bar{G} = 10^{\frac{1}{10}\bar{g}}$); i.e., $P_{T0} = P_N\gamma_0/\bar{G}$. In the presence of fading, the power needed to achieve γ_0 with outage P_{out} is $P_T = P_{T0}\bar{G}/G_{out}$. The factor $1/G_{out}$ represents the needed fixed margin.

Transmit power utilization can be improved if some knowledge of the gain is available at the transmitter. In an ideal adaptive power control scheme, the transmit power can be varied in accordance with the known fading gain G, so that the SNR is kept at the value γ_0; i.e., $\hat{P}_T = P_{T0}\bar{G}/G$. In this case, the channel never experiences outage. Extensions to the case of limited peak transmit power are possible as well, but we focus our attention on an unrestricted case for simplicity.

When the channel is not fully known, an estimate $\hat{G}$ is used in place of the true gain G and a margin K is introduced to ensure that the discrepancy between the estimated and the true channel gain does not lead to outage. The transmit power is now adjusted according to

$$\hat{P}_T = K P_{T0}\bar{G}/\hat{G} \tag{4}$$

The optimal value of K can be determined such that the requirement on P_{out} is satisfied. With the above power adaptation, outage occurs whenever the transmit power, $KP_{T0}\bar{G}/\hat{G}$, is less than the threshold $P_{T0}\bar{G}/G$. Thus, the probability of outage can be calculated as

$$P_{out} = P\{KG/\hat{G} < 1\} = P\{g - \hat{g} < -10\log K\} \tag{5}$$

Finally, we calculate the difference between the fixed and the average adjusted transmit power levels as a measure of the achievable power savings,

$$S = 10\log\frac{P_T}{\overline{\hat{P}_T}} = p_T - \overline{\hat{p}_T} \tag{6}$$

The optimal value of the margin K can be determined from the expression (5) if the statistics of the error $\varepsilon = g - \hat{g}$ are known. The error statistics depend on the specific prediction method used.

B. Prediction Methods

A trivial choice for $\hat{g}$ is to use directly the value provided by the receiver. This value, however, will be delayed by the round-trip time once it reaches the receiver. Let us denote by n the discrete instances of time separated by t_f and set the prediction lag to $t_l = t_f$ for simplicity, and let us define $g[n] = g(nt_f)$. The trivial estimate can thus be represented as $\hat{g}_0[n] = g[n-1]$. Note that we assume ideal measurements at the receiver.

If the channel gain obeys an AR process with auxiliary noise whose parameters are known, a linear predictor can be used to estimate the gain. Here, we briefly describe two cases: an AR model of order 1 and 2.

An AR(1) model is described as

$$\begin{aligned} g[n] &= \bar{g} + \Delta g[n] \\ \Delta g[n] &= a_1 \Delta g[n-1] + w[n] \end{aligned} \tag{7}$$

where $w[n]$ is the discrete-time process noise and $\bar{g}$ denotes the mean of g. Let us denote the variance of g with σ^2. Based on this model, a linear predictor of order 1 yields

$$\begin{aligned} \hat{g}_1[n] &= \bar{g} + \Delta\hat{g}_1[n] \\ \Delta\hat{g}_1[n] &= a_1 \Delta g[n-1] \end{aligned} \tag{8}$$

For an AR(1) process, the parameter a_1 is related to the Doppler frequency f_d of the channel as $a_1 = e^{-2\pi f_d |t_f|}$. The variance of the estimate and the variance of the estimation error in this case are given by

$$\begin{aligned} \sigma^2_{\hat{g}_1} &= a_1^2 \sigma^2 \\ \sigma^2_{\varepsilon_1} &= (1 - a_1^2)\sigma^2 \end{aligned} \tag{9}$$

For an AR(2) model, the gain variation is described as

$$\Delta g[n] = a_1 \Delta g[n-1] + a_2 \Delta g[n-2] + w[n] \tag{10}$$

Based on this model, the gain is estimated as

$$\begin{aligned} \hat{g}_2[n] &= \bar{g} + \Delta\hat{g}_2[n] \\ \Delta\hat{g}_2[n] &= a_1 \Delta g[n-1] + a_2 \Delta g[n-2] \end{aligned} \tag{11}$$

The parameters a_1 and a_2 are related to the parameters of the continuous-time model as

$$\begin{aligned} a_1 &= 2e^{-\xi\omega_n t_f} \cos(\sqrt{1-\xi^2}\omega_n t_f) \\ a_2 &= -e^{-2\xi\omega_n t_f} \end{aligned} \tag{12}$$

where ξ is the damping factor and $f_n = \omega_n / 2\pi$ is the natural frequency. For $\xi < 1/\sqrt{2}$, the second-order spectrum has two prominent peaks at $f_p = \pm f_n \sqrt{1 - 2\xi^2}$. The Doppler frequency, f_d, is given by

$$f_d = f_n \sqrt{(1 - 2\xi^2) + \sqrt{1 + (1 - 2\xi^2)^2}} \tag{13}$$

The variance of the estimate and the estimation error are given by

$$\begin{aligned} \sigma^2_{\hat{g}_2} &= A^2 \sigma^2 \\ \sigma^2_{\varepsilon_2} &= \left(1 - A^2\right)\sigma^2 \end{aligned} \tag{14}$$

where $A^2 = a_1^2 + a_2^2 + 2a_1^2 a_2/(1 - a_2)$.

C. Power Savings Under Log-Normal Fading

We calculate the power savings under log-normal assumption for three different estimation methods: the delayed estimate and linear prediction of order 1 and 2.

If g is log-normally distributed, Eq. (5) can be expressed in closed form as

$$P_{out} = Q\left[\frac{10\log_{10} K}{\sigma_\varepsilon}\right] \tag{15}$$

where Q denotes the Q-function, $Q(x) = \frac{1}{2}(1 - erf(x/\sqrt{2}))$. The outage probability can also be stated as

$$P_{out} = P\{G < G_{out}\} = Q[\frac{\bar{g} - 10\log G_{out}}{\sigma}] \tag{16}$$

Comparing Eqs. (15) and (16), we have that

$$K = \left[\bar{G}/G_{out}\right]^{\sigma_\varepsilon/\sigma} \tag{17}$$

where G_{out} is specified in terms of P_{out} as

$$g_{out} = \bar{g} - \sigma Q^{-1}[P_{out}] \tag{18}$$

The average transmit power needed with optimal K is

$$\overline{\hat{P}_T} = E[K P_{T0} \bar{G}/\hat{G}] = K P_{T0} 10^{\frac{\sigma^2_{\hat{g}}}{20}} \tag{19}$$

In the fixed power scenario, the average transmit power is equal to the fixed power, $P_T = P_{T0}\bar{G}/G_{out}$. Substituting for P_T and $\overline{\hat{P}_T}$, the power savings S are obtained as

$$S = \sigma Q^{-1}[P_{out}](1 - \sigma_\varepsilon/\sigma) - \frac{\sigma^2_{\hat{g}}}{2} \tag{20}$$

For linear prediction of order 1 and 2, $\sigma_{\hat{g}}$ and σ_ε are given by Eqs. (9) and (14), respectively, and the savings can thus be computed in closed form. These results can serve as an upper bound on the power savings of practical systems in which the actual model parameters are not known, and adaptive prediction is used instead.

IV. Experimental Data Processing

Rather than relying on the assumption that the fading process obeys an AR model with known parameters, we apply a linear predictor with adaptively adjusted weights a_m to the experimental data. A one-step prediction of order M is made as

$$\begin{aligned} \hat{g}_M[n] &= \hat{\bar{g}} + \Delta\hat{g}_M[n] \\ \Delta\hat{g}_M[n] &= \sum_{m=1}^{M} a_m[n] \left(g[n-m] - \hat{\bar{g}}\right) \end{aligned} \tag{21}$$

where $\hat{\bar{g}}$ is the mean estimated using an initial segment of the data. The M prediction coefficients $\{a_m\}$ are updated using an RLS algorithm based on the error $g[n] - \hat{g}_M[n]$.

Before measuring the power savings that can be achieved by prediction, we investigate the effect of various parameters on the performance of the prediction algorithm.

A. The averaging window

First, let us examine the length of the window T_w used for calculating the locally averaged values $g[n]$ that are then used to form the predictions $\hat{g}_M[n]$. If this window is too small, insufficient averaging of the instantaneous values will occur; if the window is too large, the time variation of the gain will not be well captured. To assess this trade-off, we define two types of errors. The first is the normalized averaging error, defined as

$$e_1 = \frac{\sum_{n=1}^{N} |g[n] - \tilde{g}[n]|^2}{\sum_{n=1}^{N} |\tilde{g}[n]|^2} \tag{22}$$

where N is the number of the data points. The second is the normalized prediction error, which depends on the predictor order M and is defined as

$$e_2(M) = \frac{\sum_{n=1}^{N} |\hat{g}_M[n] - g[n]|^2}{\sum_{n=1}^{N} |\tilde{g}[n]|^2} \tag{23}$$

One can also define the total error

$$e(M) = \frac{\sum_{n=1}^{N} |\hat{g}_M[n] - \tilde{g}[n]|^2}{\sum_{n=1}^{N} |\tilde{g}[n]|^2} \tag{24}$$

Using the Cauchy-Schwartz inequality, the total error is upper-bounded as

$$e(M) \leq e_u(M) = e_1 + e_2(M) + 2\sqrt{e_1 e_2(M)} \tag{25}$$

Fig. 5 illustrates the averaging error e_1 and the prediction error $e_2(M)$ versus the averaging window T_w for $t_f = 0.3$ s, 0.5 s and 1.3 s. The case $M = 0$ refers to the delayed estimate (no prediction). The figure shows that the prediction error and the averaging error exhibit opposite trends. For averaging windows longer than 2 seconds, e_1 is the dominant error. The total error in this case is mainly due to excessive smoothing of the gain variations and it cannot be noticeably reduced by increasing the order of the predictor. If the averaging window is very small, e_2 is dominant. In this case, insufficient averaging is performed, i.e. the local average tends to the instantaneous values which are changing too rapidly to be tractable via feedback. In light of these observations, $T_w = 2$ s is selected for our experimental channel.

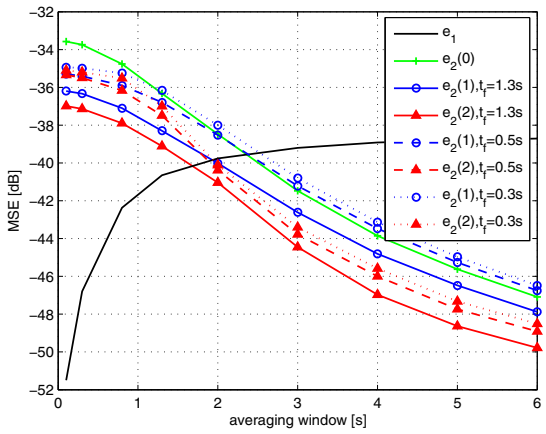

Fig. 5. *Averaging and prediction errors versus* T_w.

Fig. 5 also shows that for a fixed T_w, a greater error is observed for lower values of the feedback interval t_f. Specifically, we note that a predictor of order M achieves its best performance if the feedback interval t_f is selected to be equal to the prediction lag t_l. Accordingly, we set $t_f = t_l$ for all further processing. A relatively low feedback rate has also been reported to boost the performance of prediction in mobile radio channels [9].

B. The prediction lag and order

The major factor that fundamentally limits the performance of prediction is the round trip delay which determines the prediction lag t_l. Fig. 6 illustrates the prediction error $e_2(M)$ as a function of t_l. The averaging window is fixed at 2 seconds. As expected, the prediction error increases with prediction lag. In a practical power control system, a prediction lag of at least the channel's round-trip delay must be sustainable (1.3 s for our experimental channel).

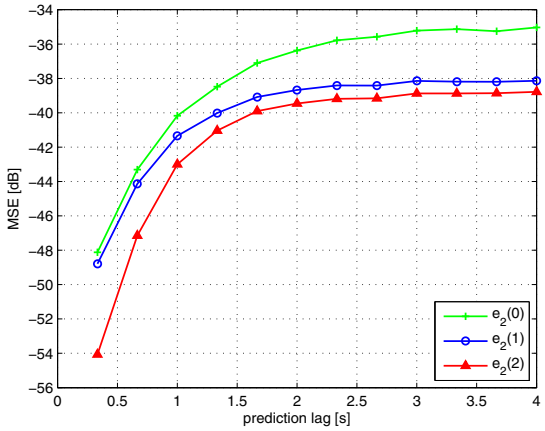

Fig. 6. *Prediction error versus* t_l. $T_w = 2$ *s.*

Results of Fig. 6 can also be used to estimate the efficiency of prediction at greater transmitter-receiver distances. For example, for a 2 km channel undergoing the same fading as our 1 km experimental channel, there is an additional 1 dB of loss due to the longer propagation delay. The order 2 and 1 predictors provide similar performance; however, the outdated estimate starts to lag considerably as the delay increases.

Finally, Fig. 7 shows the prediction error $e_2(M)$ as a function of the prediction order M for several values of the RLS forgetting factor λ. Clearly, the performance improves with prediction order. Also, among predictors of the same order, the one with the lowest forgetting factor outperforms the others. This behavior is attributed to the fact that prediction delays are long.

Although the gain in this experimental channel varies slowly enough to be predicted very well using even the outdated estimate, several dB of additional improvement is available from prediction. However, at high prediction orders, the total error is mainly due to the averaging error as the prediction error becomes negligibly small. To better clarify this fact, the upper bound on the total error (25) is also plotted in Fig. 7

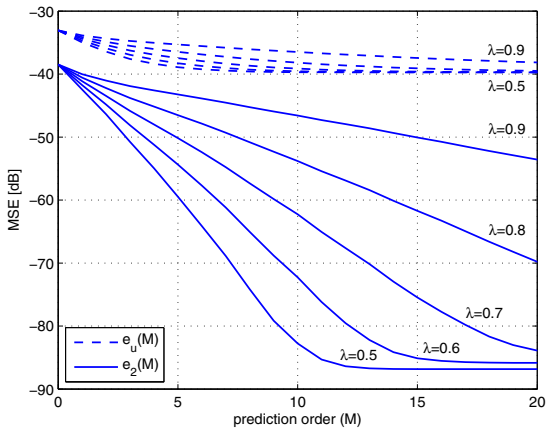

Fig. 7. *Prediction error versus the predictor order for varying forgetting factor λ of the RLS algorithm. $T_w = 2$ s and $t_l = 1.33$ s.*

(dashed line). As can be seen there, one may not expect to considerably reduce the total error by selecting a better predictor.

C. Achievable Power Savings

Fig. 8 illustrates the power consumption corresponding to the SPACE'08 recordings in several situations. If we set the minimum necessary received power so as to ensure that all transmissions in this observation interval are successful (bottom line), the total transmit power needed is P_T (top line). This power corresponds to the fixed margin case. The received power in this case ($P_R = P_T G$) is varying, exceeding the necessary minimum most of the time.

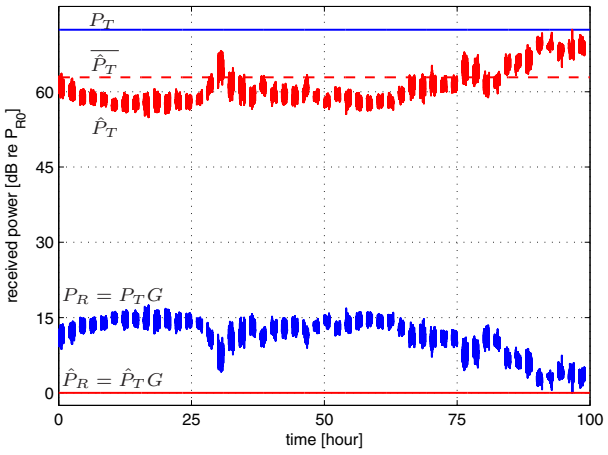

Fig. 8. *Illustration of the transmitted and received power in cases of fixed margin (P_T and P_R) and adaptive power control ($\hat{P}_T$ and $\hat{P}_R$).*

In contrast, if adaptive power control is employed, the transmit power can be adjusted to the minimum needed to ensure successful reception. In this case, the transmit power ($\hat{P}_T$) is varying, while the received power ($\hat{P}_R = \hat{P}_T G$) stays fixed (bottom line). The average transmit power consumed in this case ($\overline{\hat{P}_T}$) is shown in dashed line. The resulting savings amount to 8.7 dB.

In this example, we have assumed ideal power control to illustrate the possible savings. A practical method, based on adaptive prediction described in Section IV, will incur some penalty due to prediction lag. Note, however, that this penalty is negligible since the power varies slowly enough that prediction is almost ideal.

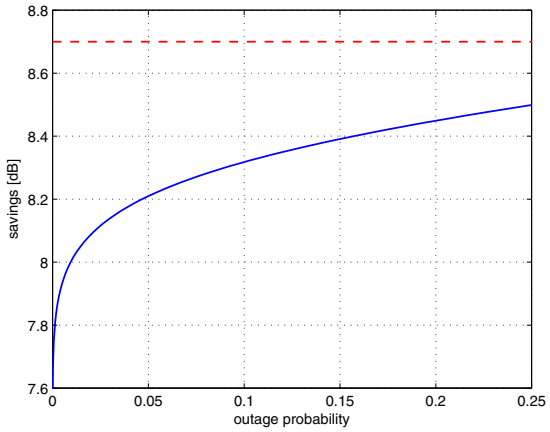

Fig. 9. *Power savings versus P_{out}.*

Using the analytical approach of Section III, the theoretical bounds on power savings are obtained assuming an AR(1) model with parameter $a_1 = 0.77$ estimated from the data. Fig. 9 illustrates the savings $p_T - \widehat{p_T}$ versus the outage probability. Note that the savings are obtained for the fixed P_T of Fig. 8. The figure shows that more savings are possible if higher outage probability is allowed. The achievable savings corresponding to ideal prediction of the gain are also plotted as a benchmark (dashed line). We note that the difference between the savings corresponding to ideal prediction and the bound obtained for the AR(1) model is less than a dB.

V. Conclusions

In this paper, the feasibility saving power by applying adaptive power control for underwater acoustic communications was investigated. Adaptive power control relies on feedback (by which the receiver informs the transmitter of the present channel state) and involves prediction of the next state (which is used to adjust the transmit power).

Experimental results are provided that support modeling of the channel gain expressed in dB as an AR process of low order (1 or 2) with Gaussian input. These observations in turn motivate the use of adaptive linear prediction for power control. Adaptive prediction using an RLS algorithm was applied to real data showing excellent performance. Analytical bounds on power savings are given under the assumption of log-normal fading with known AR parameters. The analytical bounds confirm the feasibility of achieving power savings of several dB.

Acknowledgements

This work was supported by the ONR MURI grant #N00014-07-1-0738.

REFERENCES

[1] P. Qarabaqi and M.Stojanovic, "Statistical Modeling of a Shallow Water Acoustic Communication Channel," in Proc. *Underwater Acoustic Measurements Conference*, Nafplion, Greece, Jun 2009.

[2] A. Radosevic, J. Proakis, and M. Stojanovic, "Statistical Characterization and Capacity of Shallow Water Acoustic Channels," in Proc. *IEEE Oceans Europe Conf.*, 2009.

[3] F.-X. Socheleau, J.-M. Passerieux, and C. Laot, "Characterisation of time-varying underwater acoustic communication channel with application to channel capacity," in Proc. *Underwater Acoustic Measurements Conference*, Jun 2009.

[4] W. B. Yang and T. C. Yang, "High-frequency Channel Characterization for M-ary Frequency-shift-keying Underwater Acoustic Communications," *J. Acoust. Soc. Am.*, vol. 120, no. 5, pp. 2615-2626, Nov. 2006.

[5] M. Chitre, "A High-frequency Warm Shallow Water Acoustic Communications Channel Model and Measurements," *J. Acoust. Soc. Am.*, vol. 122, no. 5, pp. 2580-2586, Nov. 2007.

[6] J. Preisig, "Acoustic Propagation Considerations for Underwater Acoustic Communications Network Development," *ACM SIGMOBILE Mobile Computing and Communications Review*, vol. 11, no. 4, pp. 2-10, Oct. 2007.

[7] R. Galvin and R.E.W. Coats, "A Stochastic Underwater Acoustic Channel Model," *OCEANS '96. MTS/IEEE.*, USA, Sep 1996.

[8] B. S. Chen, B. K. Lee, and S. K. Chen, "Adaptive Power Control of Cellular CDMA Systems via the Optimal Predictive Model," *IEEE Transactions on Wireless Communications*, vol. 4, no. 4, pp. 1914-1927, Jul 2005.

[9] A. Duel-Hallen, S. Hu, and H. Hallen, "Long-range Prediction of Fading Signals: Enabling Adaptive Transmission for Mobile Radio Channels," IEEE Signal Processing Magazine, Special Issue on Advances in Wireless and Mobile Communications, Vol. 17, No.3, pp.62-75, May 2000.

[10] M. Stojanovic and V. Chan, "Adaptive Power and Rate Control for Satellite Communications in Ka Band," in Proc. *IEEE International Conference on Communications*, 2002.

[11] B. Tomasi, P. Casari, L. Badia, and M. Zorzi, "A study of incremental redundancy hybrid ARQ over Markov channel models derived from experimental data," in Proc. *WUWNet*, Woods Hole, USA, Sep 2010.

[12] J. G. Proakis and D. G. Manolakis, *Digital Signal Processing*, 4th ed., Prentice Hall 2006.